Mitigation of photodegradation in 790nm-pumped Tm-doped fibers

G. Frith[1,*], A. Carter[2], B. Samson[2], J. Faroni[2], K Farley[2], K Tankala[2] and G. E. Town[1]

[1]*MQ Photonics Research Centre, Department of Physics and Engineering, Faculty of Science, Macquarie University, North Ryde, NSW 2109, Australia.*
[2]*Nufern, 7 Airport Park Road, East Granby, CT 06026 USA.*
**Corresponding author: gfrith@science.mq.edu.au*

ABSTRACT

The capability of Tm-doped silica fibers pumped at 790nm to efficiently produce high power emission in the 1.9~2.1µm region has been well documented to date but little has been presented on the reliability of this technology. Early experiments highlighted that photodarkening can be a significant concern when Tm-doped silica fibers are exposed to high intensity blue light. We present a discussion of the processes responsible for the production of blue light in Tm-doped fibers pumped at 790nm and how fiber composition influences these processes. Through optimization of fiber composition we have demonstrated highly efficient lasers exhibiting less than 1% output power degradation per thousand hours.

Keywords: Photodarkening, photodegradation, thulium, fiber laser

1. Background

Photodarkening (PD) of Tm-doped silica fiber was first reported by Millar *et al* in 1988 [1]. A significant reduction in the visible and infrared transmission of the fiber was observed when the fiber was exposed to high intensity light at 475nm. In those experiments, the fiber incorporated Ge which is known to be susceptible to two photon absorption near the pump wavelength [2]. For this reason, Brocklesby *et al* performed similar tests with both Tm:aluminosilicate and Tm:germanosilicate fibers to verify that the presence of Tm was indeed responsible for the observed PD [3]. Broer *et al* observed PD of Tm-doped fibers subject to infrared excitation at 1064nm which they attributed to the generation of visible and ultraviolet light through photon avalanche upconversion [4].

Although much less prominent than in fibers pumped at 1064nm, a feint blue glow can also be observed from fibers pumped at 790nm which may induce PD. Figure 1 shows spectral attenuation data supplied by Laser Zentrum Hanover for two Tm-doped fibers subject to exposure from 790nm light. The induced attenuation is in good agreement with the observations made by Brocklesby *et al* and Broer *et al*. In the fiber subject to prolonged exposure, we see that the absorption tail extends well into the near infrared region.

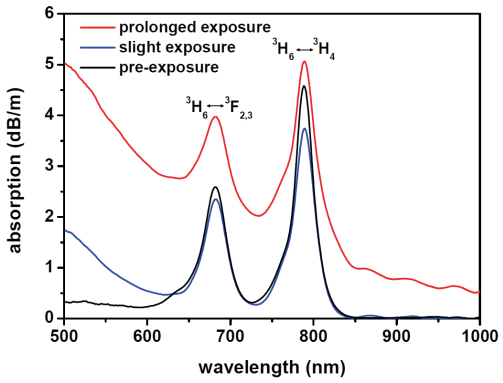

Figure 1: measured attenuation for a Tm-doped silica fiber subject to 790nm pumping.

1.1 Mechanism for production of blue light

The blue fluorescence of about 470nm seen from 790nm pumped Tm-doped fibers suggests that the transition originates from the $^1G_4$ level. A two photon avalanche upconversion process as shown in figure 2 is the most commonly accepted theory for the process responsible for the population of the $^1G_4$ level [5]. This process initially requires population of the $^3H_5$ level which predominantly occurs as a result of nonradiative decay from the $^3H_4$ level (the $^3H_5$ level may also be populated by dipole-dipole energy transfer processes [6]). Excited state absorption of 790nm photons from the $^3H_5$ level results in population of the $^1G_4$ level. As discussed by Moulton *et al* [7], excited state absorption from the $^3H_5$ level is extremely inefficient because the $^3H_5$ level rapid decays to the $^3F_4$ level. To further illustrate this point, the $^3H_5$ population (N_2) in terms of the $^3H_4$ (N_3) population may be expressed as [8]:

$$N_2 = \frac{\left(\frac{1}{\tau_{32}}+\Gamma_3\right)}{\left(\frac{1}{\tau_{21}}+\frac{1}{\tau_{20}}+\Gamma_2\right)} N_3 \qquad (1)$$

Using data presented by Walsh and Barnes [9], this implies that the $^3H_5$ population shall be approximately 0.13% of the $^3H_4$ population under steady state conditions.

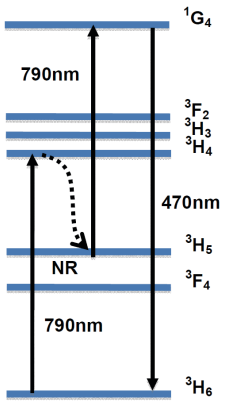

Figure 2: possible photon avalanche Upconversion scheme in Tm-doped silica.

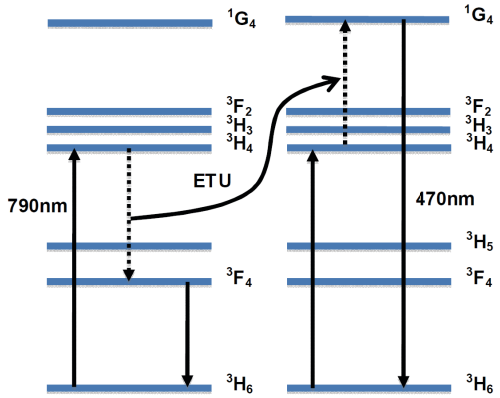

Figure 3: proposed energy transfer upconversionprocess in Tm-doped silica.

Agger and Povlsen have provided an alternate theory for the process responsible for the population of the $^1G_4$ level. They propose that population of the $^1G_4$ level may be due to a multi-phonon assisted energy transfer upconversion (ETU) process ($^3H_4$, $^3H_4 \rightarrow {}^3F_4$, $^1G_4$) as shown in figure 3 [10]. This process requires energy transfer between two adjacent Tm ions excited to the $^3H_4$ level. Energy from the de-excitation of one ion promotes the other to the $^1G_4$ level.

Due to the very low efficiency of the upconversion process, it has proven very difficult to deduce exactly which process is involved. Nevertheless, either process (ESA or ETU) depends upon initial population of the $^3H_4$ manifold. As we have observed, the rate of degradation of Tm-doped fibers can be closely linked to the $^3H_4$ population.

1.2 Lifetime of the $^3H_4$ level

The $^3H_4$, $^3H_6 \rightarrow {}^3F_4$, $^3F_4$ cross relaxation (CR) process depicted in figure 4 significantly reduces the observed lifetime of the $^3H_4$ level. This is because nonradiative energy transfer occurs at a much faster rate than the multi-phonon decay from the $^3H_4$ level. According to the Dexter model, the rate of dipole-dipole energy transfer is proportional to the sixth power of the distance between donor and accepter ions [11]. Assuming a homogeneous distribution of the Tm ions, the distance between Tm ions is proportional to the cubic root of the concentration. Accordingly, the observed lifetime can be expressed as:

$$\tau_{obs} = \frac{1}{\left(\frac{1}{\tau_{32}}+\frac{1}{\tau_{31}}+\frac{1}{\tau_{30}}+\Gamma_3+k_{CR}.n_{Tm}{}^2\right)} \quad (2)$$

Where n_{Tm} = Tm concentration in m^{-3}

The reported $^3H_4$ lifetimes for low concentration Tm-doped aluminosilicate fibers vary from around 14µs to 58µs [12, 13]. The reason for this was recently explained by Blanc *et al*; the $^3H_4$ lifetime of Tm^{3+} is closely linked to the phonon energy of the host and as such, the $^3H_4$ lifetime may range from 6µs in a pure silica environment to 110µs in a pure alumina environment [14]. To calculate k_{CR} we have assumed an observed $^3H_4$ lifetime of 28µs as the Tm concentration approaches zero (i.e. in the absence of cross relaxation). This figure is consistent with the reported lifetimes of fibers incorporating similar Al_2O_3 concentrations to those used in high Tm concentration fibers [15].

For higher concentration fibers, observed lifetimes were taken from Moulton *et al* [7] and concentrations were measured using wavelength-dispersive spectrometer microprobe analysis. The fitted value for k_{CR} was $2.7\times10^{-48}m^6s^{-1}$. We note that this value is three orders of magnitude larger than values reported for crystal hosts such as Tm:YVO4 and Tm:YAG [16,17] which is somewhat to be expected due to the higher maximum phonon energies and significant energy level broadening in silica.

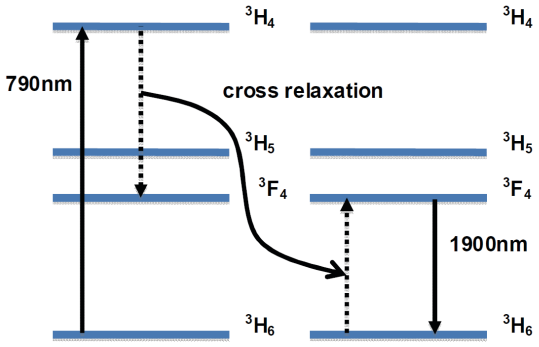

Figure 4: cross-relaxation process in Tm-doped silica.

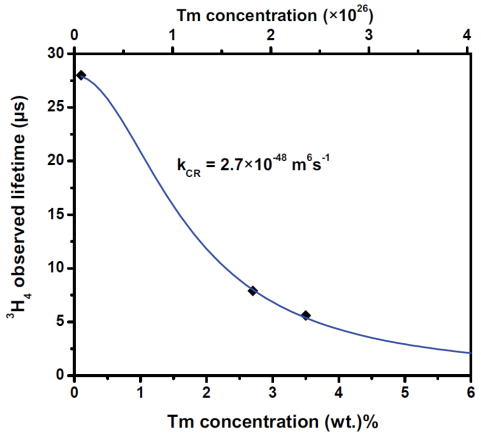

Figure 5: data used to calculate k_{CR}.

2. Experiments

To investigate the effect of Tm concentration, three single-mode aluminosilicate fibers were manufactured with Tm concentrations of 2.1, 3.3 and 4.6% and Al^{3+}/Tm^{3+} ratios of >6:1 to minimize clustering of the Tm ions [18]. Both the 2.1 and 4.6% fibers had a 10µm core with 0.15~0.16NA. In the case of the 4.6% fiber, a raised refractive index pedestal was required to lower the effective core NA [19]. The 3.3% fiber had an 8µm core with 0.2NA. To achieve efficient pump mode scrambling, claddings were either octagonal shaped (oct.) or incorporated *panda*-type stress rods (PM). Properties of the fibers are summarized in table 1.

Table 1: summary of properties of tested fibers

Parameter	Unit	Fiber		
		1	2	3
Tm concentration	(wt.)%	2.1	3.3	4.6
Al/Tm ratio	-	10:1	9.6:1	7.1:1
Core diameter	µm	10	8	10
Clad diameter	µm	130 (PM)	130 (oct.)	130 (PM)
Coating diameter	µm	250	250	250
Core NA	-	0.15	0.2	0.16 (eff)

2.1 Efficiency characterization

Each fiber was tested in a linear laser cavity consisting of a fiber Bragg grating (FBG) at one end and the Fresnel reflection from the cleaved fiber facet at the other as shown in figure 6. The FBG was written in a photosensitive fiber with a 10µm 0.16NA core and 130µm 0.45NA cladding. It had a peak reflectivity of >95% at 1.95µm. A pump source that delivered up to 50W at 792nm into a 125µm 0.45NA fiber was used to end-pump the laser cavity. A silicon filter was used to block any residual (unabsorbed) pump light at the output of the laser.

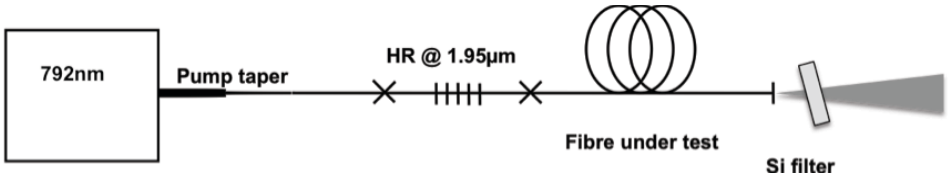

Figure 6: configuration used to test performance of Tm-doped fibers

Output powers were measured with and without the silicon filter inserted to precisely determine the residual pump power. These measurements were used to calculate the normalized core absorption (i.e. absorption in dB/m with respect to 1% Tm) which is an indication of the CR efficiency since CR increases ground state depletion. The performance of each fiber is shown in table 2. Normalized core absorption and slope efficiency for each fiber is also plotted in figure 7.

Table 2: summary of measured properties and performance of tested fibers

Parameter	Unit	Fiber		
		1	2	3
Tm concentration	(wt.)%	2.1	3.3	4.6
Fiber length	m	4	6.5	2.65
Slope eff. (rel. launched)	%	48.6	57.2	57.4
Slope eff. (rel. absorbed)	%	54.7	60.1	63.8
Threshold	W	2.31	2.92	1.81
Pump abs @ 40A	dB	9.53	13.5	10.0
Pump power @ 20W output	W	43.5	37.9	36.7
Normalised core abs'n	dB/Tm%m	196	159	138

As we can see from table 2, increasing the Tm-concentration from 2.1% to 4.6% resulted in a 17% increase in absorbed slope efficiency. In addition to this we notice that the 4.6% fiber had around 30% lower normalized core absorption than the 2.1% fiber.

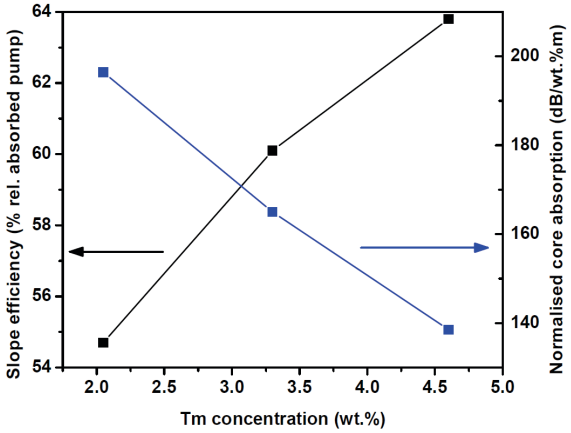

Figure 7: measured absorbed slope efficiency and normalized core attenuation for fibers ranging from 2.1 to 4.6% Tm

2.3 Degradation measurements

To measure degradation, each laser was placed in an enclosed chamber within an environmentally controlled laboratory to ensure stable operating conditions for the laser. The active (Tm-doped) fiber was conductively cooled by an aluminum mandrel which was maintained at a constant temperature along with the pump diode and laser power meter.

Each fiber laser was started with a nominal output power of 20W. The output power was recorded every 10 seconds. Figure 9 shows an example of data collected from a test. After allowing for initial settling of the system, a line of best fit was applied to the recorded data. The results are shown in terms of percent degradation per thousand hours in figure 10. As shown by figure 9, degradation decreased with increasing Tm concentration. The 2.1% Tm fiber showed 13.8% degradation per 1000 hours. Increasing the Tm concentration to 3.3% resulted in a 240% drop in degradation. The 4.6% Tm fiber showed negligible (0.2%) degradation which we considered to be less than the minimum resolution of the test. Nevertheless, if we consider the device lifetime to be the time taken to reach 10% output power degradation; these results indicate that device lifetimes exceeding 10 thousand hours are feasible.

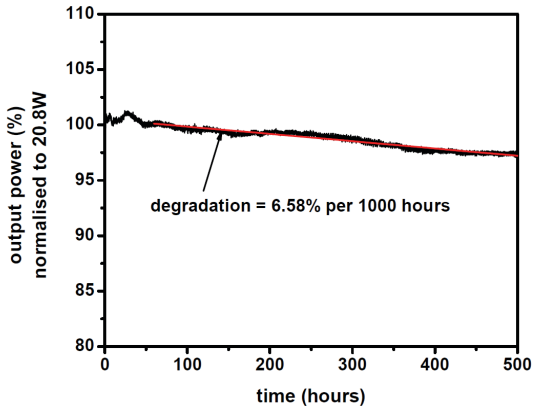

Figure 8: example degradation test data for laser.

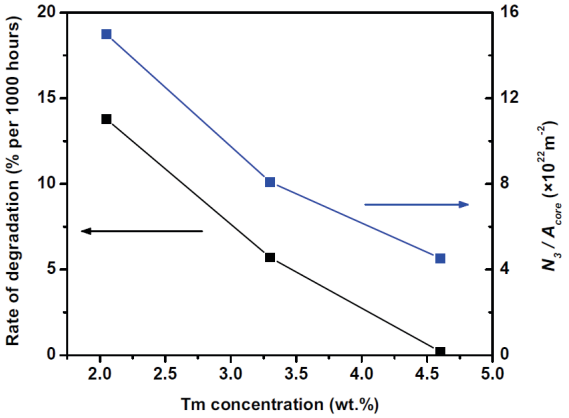

Figure 9: degradation and $^3H_4$ population / core area versus Tm concentration.

3. Discusison

3.1 Laser modeling

To determine the $^3H_4$ population we have generated a model based on the Wilcox model [8]. Accounting for the $^3H_4$, $^3H_6 \rightarrow {}^3F_4$, $^3F_4$ cross relaxation (CR) process, the rate equations along the length of the fiber can be expressed as:

$$\frac{dN_3}{dt} = \frac{\sigma_a^p P_p N_0}{h\nu_p A_{clad}} \cdot \frac{A_{core}}{A_{clad}} - \frac{N_3}{\tau_{32}} - \frac{N_3}{\tau_{31}} - \frac{N_3}{\tau_{30}} - \Gamma_3 N_3 - \frac{N_3 N_0 k_{CR} {n_{Tm}}^2}{N_{total}} \tag{3}$$

$$\frac{dN_2}{dt} = \frac{N_3}{\tau_{32}} - \frac{N_2}{\tau_{21}} - \frac{N_2}{\tau_{20}} - \Gamma_2 N_2 \tag{4}$$

$$\frac{dN_1}{dt} = \frac{N_3}{\tau_{31}} + \frac{N_2}{\tau_{21}} + \frac{2N_3 N_0 k_{CR} {n_{Tm}}^2}{N_{total}} - \frac{N_1}{\tau_{10}} - \Gamma_1 N_1 - \frac{\sigma_e^s N_1 P_s}{h\nu_s A_{eff}} \cdot \frac{A_{eff}}{A_{core}} + \frac{\sigma_a^s N_0 P_s}{h\nu_s A_{eff}} \cdot \frac{A_{eff}}{A_{core}} \tag{5}$$

$$\frac{dN_0}{dt} = \frac{N_3}{\tau_{30}} + \frac{N_2}{\tau_{21}} + \frac{N_1}{\tau_{10}} + \Gamma_1 N_1 + \frac{\sigma_e^s N_1 P_s}{h\nu_s A_{eff}} \cdot \frac{A_{eff}}{A_{core}} - \frac{\sigma_a^s N_0 P_s}{h\nu_s A_{eff}} \cdot \frac{A_{eff}}{A_{core}} - \frac{\sigma_a^p N_0 P_p}{h\nu_p A_{clad}} \cdot \frac{A_{core}}{A_{clad}} - \frac{N_3 N_0 k_{CR} {n_{Tm}}^2}{N_{total}} \tag{6}$$

As previously discussed, N_2 is sufficiently small compared to the other levels to be ignored, therefore we assume:

$$N_{total} = N_0 + N_1 + N_3 \quad (7)$$

Through solving the above equations and some degree of algebraic manipulation, the populations in steady state may be expressed as:

$$N_3(z) = \frac{\alpha N_0(z)}{1+\beta N_0(z)} \quad (8)$$

$$N_1(z) = \frac{AN_0(z)+BN_0(z)^2}{1+\beta N_0(z)} \quad (9)$$

$$N_0(z) = \frac{B(z)N_{total}-1-A(z)-\alpha(z)+\sqrt{(B(z)N_{total}-1-A(z)-\alpha(z))^2+4(B(z)+\beta)N_{total}}}{2(B(z)+\beta)} \quad (10)$$

Where:

$$\alpha(z) = \frac{\sigma_a^p P_p(z) A_{core}}{h\nu_p (A_{clad})^2 + \left(\frac{1}{\tau_{32}}+\frac{1}{\tau_{31}}+\frac{1}{\tau_{30}}+\Gamma_3\right)} \quad (11)$$

$$\beta = \frac{k_{CR} {n_{Tm}}^2}{N_{total}\left(\frac{1}{\tau_{32}}+\frac{1}{\tau_{31}}+\frac{1}{\tau_{30}}+\Gamma_3\right)} \quad (12)$$

$$A(z) = \frac{\alpha(z)\left(\frac{1}{\tau_{31}}+\frac{\sigma_a^S P_S}{h\nu_S A_{core}}\right)}{\left(\frac{1}{\tau_{10}}+\Gamma_1+\frac{\sigma_e^S P_S}{h\nu_S A_{core}}\right)} \quad (13)$$

$$B(z) = \frac{\alpha(z)\left(\frac{2k_{CR}{n_{Tm}}^2}{N_{total}}+\frac{\sigma_a^S P_S}{\alpha h\nu_S A_{core}}\right)}{\left(\frac{1}{\tau_{10}}+\Gamma_1+\frac{\sigma_e^S P_S}{h\nu_S A_{core}}\right)} \quad (14)$$

$$\frac{dP_p}{dz} = -\sigma_a^p N_0(z) P_p(z) \quad (15)$$

$$P_S = \frac{P_{output}}{(1-R_1R_2)} \quad (16)$$

The fiber parameters used to model the lasers are as shown in table 1; spectroscopic parameters are shown in table 3.

Table 3. Spectroscopic parameters used in laser model

Parameter	Value	Source
τ_{32}	0.052029s	[9]
τ_{31}	0.008253s	[9]
τ_{30}	0.000772s	[9]
τ_{10}	0.004559s	[9]
Γ_3	34278.66s	[9],[15]
Γ_1	1563.171 s^{-1}	[7],[9]
k_{CR}	2.7×10^{-48} m^6s^{-1}	This report
σ_a^p	$8.5\times10^{-25}m^2$	[12]
σ_e^s	4×10^{-25} m^2	[9]
σ_a^s	2×10^{-27} m^2	This report*

*The value for σ_a^s was adjusted for best correlation with measured laser performance

For photon avalanche upconversion, the intracore intensity of the blue fluorescence shall be proportional to the average $^3H_4$ population divided by the core cross section; that is:

$$I_{blue} \propto \frac{1}{A_{core}} \int_0^l N_3(z).dz \tag{17}$$

For each of the fibers we have shown $\overline{N_3}/A_{core}$ in figure 9. As we can see, there is a clear correlation between this value and the measured rate of degradation.

Although some blue fluorescence was visible from the 4.6% fiber (albeit much dimmer than the 2.1% fiber), the measured PD was negligible. This is evidence that factors such thermal bleaching or photobleaching may also play a significant role in determining the rate of PD for Tm-doped fibers. Photobleaching has previously been observed in both Tm:silica and Tm:ZBLAN fibers [3,20]. Millar *et al* reported observations of thermal bleaching above 350°C [1] but as we show in section 3.2, these temperatures are well above the normal operating core temperatures of our lasers.

3.2 Thermal management

We have shown that one method to reduce PD in 790nm-pumped Tm-doped fibers is to increase the Tm concentration. Intuitively, increasing the Tm concentration should likewise increase the thermal loading of the fiber. Taking the measured performance of the 2.1 and 4.6% fibers we have modeled the maximum fiber temperature assuming thermal conductivities of 1.35W/mK for silica and 0.17W/mK for the polymer coating. Figure 10 shows the modeled maximum temperatures for the lower (2.1%) and higher (4.6%) concentration fibers operating at 20W output power. In addition to this, we have shown the modeled maximum temperature for the higher concentration fiber operating at 50W output power.

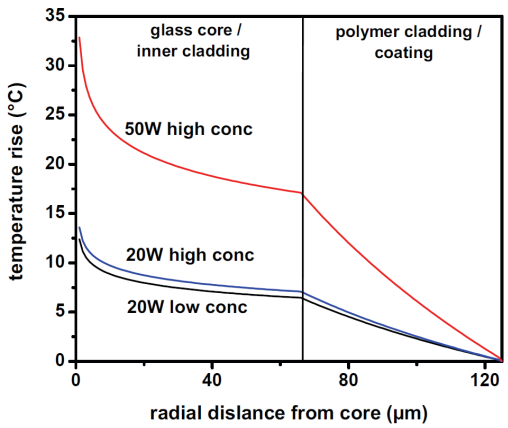

Figure 10: modeled maximum temperature profile for 2.1% Tm (low conc) and 4.6% Tm (high conc) fibers operating at 20 and 50W

Figure 10 indicates that even though the Tm concentration was more than doubled, the difference in maximum temperatures at the glass/polymer interface was only of the order of a few degrees Celsius. The reason for this is twofold – firstly, the higher efficiency of the higher concentration fiber resulted in less pump power being required to achieve the nominal output of 20W. Secondly, as previously discussed, the greater CR efficiency of higher concentration fibers results in increased ground state depletion; hence, the ground state absorption is not proportional to the fiber concentration.

To date we have demonstrated up to 66W output at 1920nm from a simple end-pumped linear cavity laser using the 4.6% Tm single mode fiber [21]. We believe that further power scaling of this architecture was largely limited by thermal management issues. One solution to decrease the thermal load is to simply reduce the core diameter but this is only practical if the desired wavelength of operation is greater than about 1.95µm. For wavelengths shorter than 1.95µm,

a relatively large core to clad ratio must be maintained to limit reabsorption effects. Another solution is to use large mode area (LMA) fibers but as we have previously demonstrated, single mode fibers are able to achieve better conversion efficiency than large mode area (LMA) fibers [22].

To facilitate further power scaling of single mode fiber architectures without sacrificing reliability we are currently investigating two possible options. The first option is utilizing ring doping to decrease cladding absorption without affecting efficiency at shorter wavelengths. The second method is a novel technique of increasing the local ion concentration whilst maintaining a low average concentration through nanoparticle deposition [23].

3.3 Alternative host compositions

Methods for mitigating PD may also involve adopting alternative host compositions. High Al^{3+} concentrations have traditionally been incorporated into Tm-doped fibers to minimize clustering of the Tm ions. Clustering leads to $^3F_4$, $^3F_4 \rightarrow {}^3H_6$, $^3H_4$ ETU which is detrimental to laser performance [24]. Blanc *et al* showed that the use of high Al^{3+} concentrations results in enhancement of the $^3H_4$ lifetime [14] which we have shown here is disadvantageous for fiber reliability.

Incorporation of phosphorus has been shown to decrease PD in Yb-doped fibers [25]. In addition to this, incorporating P_2O_5 increases the maximum phonon energy of silica which should reduce the $^3H_4$ lifetime. Unfortunately P_2O_5 also significantly influences the spectroscopy of the $^3F_4$ upper laser level. In experiments with Tm:phosphosilicate fiber we have observed an increase in the laser threshold from ~2W to 20W indicating an unacceptable decrease in the gain for the $^3F_4 \rightarrow {}^3H_6$ transition. It is possible that an alumino-phosphosilicate host may facilitate lower PD without overly diminishing gain at ~2μm.

4. Conclusions

Photodarkening of Tm-doped fibers pumped at 790nm occurs as a result of an upconversion process leading to the production of blue light at ~470nm. The rate of upconversion can be linked to the $^3H_4$ population. Within this report we have also shown here that the rate of photodegradation is proportional to the population of the $^3H_4$ level.

Because cross-relaxation depopulates the $^3H_4$ level, we have provided evidence that optimizing of the cross-relaxation process through using relatively high Tm concentrations assists in minimizing upconversion and PD. Using a single mode fiber with 4.6 (wt)% Tm we demonstrated a 20W 1.95μm laser exhibiting a rate of degradation of less than 10% per 10 thousand hours. These results validate the viability of 790nm pumped Tm-doped fiber technology for applications which demand highly reliable operation.

Acknowledgements

The authors would like to thank Frithjof Haxsen from Laser Zentrum Hannover for supplying the spectral data presented in figure 1.

References

[1] Millar, C. A., Mallinson, S. R., Ainslie, B. J. and Craig, S. P., "Photochromic behaviour of thulium-doped silica optical fibers," Electronics Letters 24, 590-591 (1998)
[2] Lam, D. K. W. and Garside, B. K., "Characterization of single-mode optical fiber filters," Applied Optics 20, 440-445 (1981)
[3] Brocklesby, W. S., Mathieu, A., Lincoln, J. R. and Brown, R. S., "Defect production in silica fibers doped with Tm^{3+}," Optics Letters 18, 2105 (1993)
[4] Broer, M. M., Krol, D. M. and DiGiovanni, D. J., "Highly nonlinear near-resonant photodarkening in a thulium-doped aluminosilicate glass fiber," Optics Letters 18, 799–801 (1993)
[5] Agger, S., Povlsen, J. H. and Varming, P., "Single-frequency thulium-doped distributed-feedback fiber laser," Optics Letters 29, 1503-1505 (2004)

[6] Jackson, S. D., "Cross relaxation and energy transfer upconversion processes relevant to the functioning of 2μm Tm^{3+}-doped silica fibre lasers," Optics Communications 230, 197-203 (2004)
[7] Moulton, P. F., Rines, G. A., Slobodtchikov, E. V., Wall, K. F., Frith, G., Samson, B and Carter, A. L. G, "Tm-doped fiber lasers:fundamentals and power scaling," IEEE J. Selected Topics in Quantum Electronics 15, 85-91 (2009)
[8] Wilcox, P., "Model of Thulium Doped Double Clad Fibers Pumped at 795nm," unpublished.
[9] Walsh, B. M. and Barnes, N. P., "Comparison of Tm:ZBLAN and Tm:silica fiber lasers; Spectroscopy and tunable pulsed laser operation around 1.9μm," Applied Physics B 78, 325-333 (2004)
[10] Agger, S. and Povlsen, J. H., "Emission and absorption cross section of thulium doped silica fibers," Optics Express 14, 50-57 (2006)
[11] Dexter, D. L., "A Theory of Sensitized Luminescence in Solids," J. Chem. Phys. 21(5), 836-850 (1953)
[12] Jackson, S D. and King, T. A., "Theoretical Modeling of Tm-Doped Silica Fiber Lasers," J. Lightwave Tech. 17(5), 948-956 (1999)
[13] Peterka, P., Kašík, I., Matějec, V., Blanc, W., Faure, B., Dussardier, B., Monnom, G. and Kubeček, V., "Thulium-doped silica-based optical fibers for cladding-pumped fiber amplifiers," Optical Materials 30(1), 174-176 (2007)
[14] Blanc, W., Sebastian, T.L., Dussardier, B., Michel, C., Faure, B., Ude, M. and Monnom, G., "Thulium environment in a silica doped optical fibre," J. Non-Cryst. Solids 354(2-9), 435-439 (2008)
[15] Simpson, D. A., Gibbs, W. E. K., Baxter, G. W., Collins, S. F., Blanc, W., Dussardier B. and Monnom, G., "Energy transfer up-conversion in Tm^{3+} -doped silica fibre," J. Non-Cryst. Solids 352, 136-141 (2006)
[16] Bettinelli, M., Ermeneux, F. S., Moncorge, R. and Cavalli, E., "Fluorescence dynamics of YVO_4:Tm^{3+}, YVO_4:Tm^{3+}, Tb^{3+} and YVO_4:Tm^{3+}, Ho^{3+} crystals" Journal Physics: Condensed Matter 10, 8207 (1998)
[17] Armagan G., Buoncristiani A. M. and DiBartolo B., "Excited state dynamics of thulium ions in Yttrium Aluminum Garnets," Optical Mater. 1(1), 11-20 (1992)
[18] Ainslie, B. J., Craig, S. P. and Davey, S. T., "The fabrication and optical properties of Nd^{3+} in silica-based optical fibers," Materials Letters 5, 143-146 (1987)
[19] Tankala, K., Samson, B., Carter, A., Farroni, J., Machewirth, D., Jacobson, N., Sanchez, A., Galvanauskas, A., Torruellas, W. and Chen, Y., "New Developments in High Power Eye-Safe LMA Fibers," Proc. SPIE 6102, paper 6102-06 (2006)
[20] Chandonnet, A., Laperle, P., LaRochelle, S. and Vallée, R., "Photodegradation of fluoride glass blue fiber laser," Proc. SPIE 2998, 70-81 (1997)
[21] Christensen, S., Frith, G., Samson, B., Carter, A., Farroni, J., Farley, K. and Tankala, K., "Efficient and reliable 790nm-pumped Tm lasers from 1.91 to 2.13μm," in Proc. SSDLTR, Albuquerque, 2-5 June (2008)
[22] Frith, G. Carter, A. Samson, B. Town, G., "Design considerations for short-wavelength operation of 790-nm-pumped Tm-doped fibers," Applied Optics 48, 5072-5075 (2009).
[23] Kucera, C., Kokuoz, B., Edmondson, D., Griese, D., Miller, M., James, A., Baker, W. and Ballato, J., "Designer emission spectra through tailored energy transfer in nanoparticle-doped silica performs," Optics Letters 34(15), 2339-2341 (2009)
[24] Jackson, S. D and Mossman, S., "Efficiency dependence on the Tm^{3+} and Al^{3+} concentrations for Tm^{3+}-doped silica double-clad fiber lasers", Applied Optics 42, 2702-2707 (2003)
[25] Shubin, A.V., Yashkov, M.V., Melkumov, M.A., Smirnov, S.A., Bufetov, I.A. and Dianov, E.M., "Photodarkening of alumosilicate and phosphosilicate Yb-doped fibers," in Proc. European Conference on Lasers and Electro-Optics, Munich, 17-22 June (2007)